
Since January 2020 Elsevier has created a COVID-19 resource centre with free information in English and Mandarin on the novel coronavirus COVID-19. The COVID-19 resource centre is hosted on Elsevier Connect, the company's public news and information website.

Journal of Ginseng Research xxx (xxxx) xxx

Contents lists available at ScienceDirect

Journal of Ginseng Research

journal homepage: www.sciencedirect.com/journal/journal-of-ginseng-research

# Production and characterization of lentivirus vector-based SARS-CoV-2 pseudoviruses with dual reporters: Evaluation of anti-SARS-CoV-2 viral effect of Korean red ginseng

Jeonghui Moon [a], Younghun Jung [a], Seokoh Moon [a], Jaehyeon Hwang, Soomin Kim, Mi Soo Kim, Jeong Hyeon Yoon, Kyeongwon Kim, Youngseo Park, Jae Youl Cho[**], Dae-Hyuk Kweon[*]

*Department of Integrative Biotechnology, College of Biotechnology and Bioengineering, Sungkyunkwan University, Suwon, 16419, Republic of Korea*

ARTICLE INFO

*Article history:*
Received 2 May 2022
Received in revised form
8 July 2022
Accepted 11 July 2022
Available online xxx

*Keywords:*
SARS-CoV-2
pseudovirus
dual reporters
antiviral
lentivirus
Korean red ginseng

ABSTRACT

*Background:* Pseudotyped virus systems that incorporate viral proteins have been widely employed for the rapid determination of the effectiveness and neutralizing activity of drug and vaccine candidates in biosafety level 2 facilities. We report an efficient method for producing severe acute respiratory syndrome coronavirus 2 (SARS-CoV-2) pseudovirus with dual luciferase and fluorescent protein reporters. Moreover, using the established method, we also aimed to investigate whether Korean red ginseng (KRG), a valuable Korean herbal medicine, can attenuate infectivity of the pseudotyped virus.

*Methods:* A pseudovirus of SARS-CoV-2 (SARS-2pv) was constructed and efficiently produced using lentivirus vector systems available in the public domain by the introduction of critical mutations in the cytoplasmic tail of the spike protein. KRG extract was dose-dependently treated to Calu-3 cells during SARS2-pv treatment to evaluate the protective activity against SARS-CoV-2.

*Results:* The use of Calu-3 cells or the expression of angiotensin-converting enzyme 2 (ACE2) in HEK293T cells enabled SARS-2pv infection of host cells. Coexpression of transmembrane protease serine subtype 2 (TMPRSS2), which is the activator of spike protein, with ACE2 dramatically elevated luciferase activity, confirming the importance of the TMPRSS2-mediated pathway during SARS-CoV-2 entry. Our pseudovirus assay also revealed that KRG elicited resistance to SARS-CoV-2 infection in lung cells, suggesting its beneficial health effect.

*Conclusion:* The method demonstrated the production of SARS-2pv for the analysis of vaccine or drug candidates. When KRG was assessed by the method, it protected host cells from coronavirus infection. Further studies will be followed for demonstrating this potential benefit.



## 1. Introduction

Effective drugs and vaccines are required to treat and prevent infections caused by both emerging and re-emerging viruses. However, the handling of highly pathogenic viruses such as severe acute respiratory syndrome coronavirus 2 (SARS-CoV-2), Middle East respiratory syndrome coronavirus (MERS-CoV), avian influenza, and Ebola requires biosafety level-3 or -4 laboratories. This is a major hurdle for the development of vaccines and drugs against viruses. The use of pseudoviruses helps avoid the handling of infectious viruses, thus facilitating drug development in lower biosafety level facilities [1,2]. Pseudoviruses have been used in the detection and testing of neutralizing antibodies against various viruses [3–9]. Furthermore, pseudoviruses serve as alternatives to test vaccines, thus eliminating one of the major limitations in vaccine development [10–13]. Among the many viruses, vesicular stomatitis virus (VSV) and lentivirus vectors are the most utilized

*Abbreviations:* NiV, Nipah virus; MARV, Marburg virus; CHIKV, chikungunya virus; LASV, lassa mammarenavirus; HEK293T, human embryonic kidney 293T; SDS, sodium dodecyl sulfate; SDS-PAGE, sodium dodecyl sulfate-polyacrylamide gel electrophoresis; IgG, immunoglobulin G; EGFP, enhanced green fluorescent protein.

* Corresponding author.
** Corresponding author.
*E-mail addresses:* jaecho@skku.edu (J.Y. Cho), dhkweon@skku.edu (D.-H. Kweon).

[a] Equal contribution.

https://doi.org/10.1016/j.jgr.2022.07.003


Please cite this article as: J. Moon, Y. Jung, S. Moon *et al.*, Production and characterization of lentivirus vector-based SARS-CoV-2 pseudoviruses with dual reporters: Evaluation of anti-SARS-CoV-2 viral effect of Korean red ginseng, Journal of Ginseng Research, https://doi.org/10.1016/j.jgr.2022.07.003

[14] owing to their rapid production rate and non-pathogenicity [3,15,16]. Lentivirus vectors, mostly derived from human immunodeficiency virus type 1 (HIV-1), have been employed to generate pseudoviruses for NiV [10], MARV [17], CHIKV [18], and certain influenza viruses [3,15]. In addition, SARS-CoV-2 [19–21], MERS-CoV [4,22], SARS-CoV [23,24], Ebola [25], and LASV [26,27] pseudoviruses have been produced using both lentivirus and VSV-ΔG pseudovirus systems.

Coronaviruses (CoVs) are enveloped viruses containing positive-sense, single-stranded RNA. They can infect various natural hosts depending on their subtype [28]. SARS-CoV-2 enters host cells through affinity between the S1 unit of the spike protein and angiotensin-converting enzyme 2 (ACE2) on the cell surface [29,30]. The cellular protease, transmembrane protease serine subtype 2 (TMPRSS2), is essential for the cleavage of the ACE2-bound spike protein at the S1/S2 interface, which activates it to a fusion-inducible state and enables the robust infection of lung cells [31,32]. Cleavage of the SARS-CoV-2 S protein to S1 and S2 increases the efficiency of viral entry, and determines virus infectivity [19,22,33–36]. Thus, the spike protein is a viable and ideal target for the development of vaccines and therapeutics and therefore is often combined with a pseudovirus vector. To date, several pseudoviruses of SARS-CoV-2 (SARS-2pv) have been reported [7,19,31,37–41]. However, a majority of the SARS-2pvs have been produced only at low titers. Furthermore, most SARS-2pvs express a single reporter gene, such as either a fluorescence protein or a firefly luciferase reporter, whereas a dual reporter system simultaneously expressing both fluorescent protein and luciferase provides many useful features. Recently, two SARS-2pvs with dual reporter systems have been reported, one based on VSVΔG and the other based on lentivirus [31,42]. In case of SARS-2pv, lentiviral vectors have several advantages over VSV-based vectors. First, lentiviruses possess a large transgene capacity that enables the expression of large or multicistronic genes in target cells. Second, it can efficiently infect and integrate its genome into both dividing and non-dividing cells. Finally, lentivirus-based SARS-2pv is a spherical particle similar to the native SARS-CoV-2, whereas VSV-based SARS-2pv is bullet-shaped and displays different shapes and distributions of spike proteins compared to native SARS-CoV-2 [43,44].

In this study, we constructed dual reporter systems with robust infectivity using plasmids available in public domains, such as Addgene. Lentivirus vector systems (pNL4.3, pCMVR8.74, and pHIV-EGFP-Luc) available in the public domain were tested for packaging efficiency using vesicular stomatitis virus G glycoprotein (VSV-G) before the construction of SARS-2pv using a spike protein. The two-plasmid system comprising genes for packaging as well as dual reporters in a single vector and VSV-G in the other vector showed 100-fold higher luciferase activity compared with that of the the three-plasmid system, which harbors the packaging and reporter genes in separate plasmids. The SARS-2pv is composed of a two-plasmid system and was constructed with a plasmid encoding the SARS-CoV-2 spike protein. Luciferase activity and fluorescence intensity showed strong correlations, confirming the compatibility of the two different reporters. In addition to the demonstration of host cell-dependent infectivity of SARS-2pv, we also demonstrated that chemical inhibitors against SARS-CoV-2 showed activity comparable to previous results obtained with live viruses, and Korean red ginseng (KRG) induced host cell resistance to SARS-2pv infection. Moreover, mutations facilitating viral entry elevate SARS-2pv infectivity. Our simple and efficient production of SARS-2pv is useful for assessing the activity of vaccines and drug candidates for SARS-CoV-2 (Fig. 1A).

## 2. Materials and methods

### 2.1. Cells and plasmids

Calu-3, HEK293T, and Vero cell lines were obtained from the Korean Cell Line Bank (KCBL, Seoul, Korea). Calu-3 and Vero cell lines were cultured in Dulbecco's modified Eagle's medium (DMEM) with 10% fetal bovine serum (FBS), and 100 U/mL penicillin, streptomycin, and fungizone at 37 °C in 5% $CO_2$. HEK293T cells were cultured in DMEM with 10% FBS, and 100 U/mL penicillin, streptomycin, and neomycin at 37 °C in 5% $CO_2$.

The plasmid pNL4.3-mCherry-Luciferase was a gift from Dr. Warner Greene (Addgene plasmid # 44965; http://n2t.net/addgene:44965; RRID: Addgene_44965). Plasmid pCMVR8.74 was a gift from Dr. Didier Trono (Addgene plasmid # 22036; http://n2t.net/addgene:22036; RRID: Addgene_22036). The plasmid pHIV-EGFP-Luciferase was a gift from Dr. Bryan Welm (Addgene plasmid # 21375; http://n2t.net/addgene:21375; RRID: Addgene_21375). Plasmids pCMV-ACE2, pCMV-TMPRSS2, and the full-length codon-optimized S gene from SARS-CoV-2 (previously 2019-nCoV-2, S WT) in the pCMV vector were obtained from Sino Biological, Inc. (Beijing, China). Plasmids pCMV-VSV-G and pCMV-mVSV-G (H162R mutant) were kindly provided by the Korea Institute of Science and Technology (KIST, Seoul, Korea). The plasmid pS-CTΔ (a mutant S protein with a C-terminal 'KxHxx' motif for cytoplasmic tail mutation) was generated using the primers 5′-TGCTGAAAGGAGTGGCACTGGCCTACACCTGAATCT-3′ and 5′-AGATTCAGGTGTAGGCCAGTGCCACTCCTTTCAGCA-3′ [45]. The plasmid pS-L452R (a mutant S protein with a C-terminal 'KxHxx' motif mutation and L452R) was generated using the primers 5′-GGCAACTACAACTACCGGTACAGACTGTTCAGG-3′ and 5′-CCTGAACAG-TCTGTACCGGTAGTTGTAGTTGCC-3′. The plasmid pS-E484Q (a mutant S protein with a C-terminal 'KxHxx' motif mutation and E484Q) was generated using the primers 5′-CCATG-TAATGGAGTGCAGGGCTTCAACTGTTAC-3′ and 5′-GTAACAGTTGAAGCCCTGCACTCCATTACATGG-3′. The plasmid pS-E484Q + L452R dual mutant was generated using both E484Q and L452R primers.

### 2.2. Generation of transient 293T-ACE2 and 293T-ACE2-TMPRSS2

Transient HEK293T-ACE2 and HEK293T-ACE2-TMPRSS2 cells were generated by transfection with pCMV-ACE2 or co-transfection with pCMV-ACE2 and pCMV-TMPRSS2 plasmids, respectively. Briefly, $4 \times 10^6$ HEK293T cells were transfected with each plasmid using polyethyleneimine (PEI) MAX transfection reagent (Polysciences, Warrington, USA) according to the manufacturer's instructions. These transient 293T-ACE2 and 293T-ACE2-TMPRSS2 cells were cultured in DMEM with 10% FBS, 100 mg/mL streptomycin, 100 unit/mL penicillin, and 100 mg/mL hygromycin at 37 °C in 5% $CO_2$. The expression of ACE2 and TMPRSS2 was confirmed using western blotting.

### 2.3. Production and titration of pseudotyped viruses

To generate VSVpv using a two-plasmid system, $4 \times 10^6$ HEK293T cells were co-transfected with 10 μg pNL4.3-mCherry-Luciferase and 10 μg pCMV-VSV-G using the PEI MAX transfection reagent. For the three-plasmid system, 10 μg of pCMVR8.74, 10 μg of pHIV-EGFP-Luciferase, and 10 μg of pCMV-VSV-G were co-transfected. For the production of SARS-2pv, 10 μg of pNL4.3-mCherry-Luciferase and 10 μg of plasmids encoding SARS-CoV-2 spike protein (pS-WT, pS-CTMut, pS-CTMut L452R, pS-CTMut

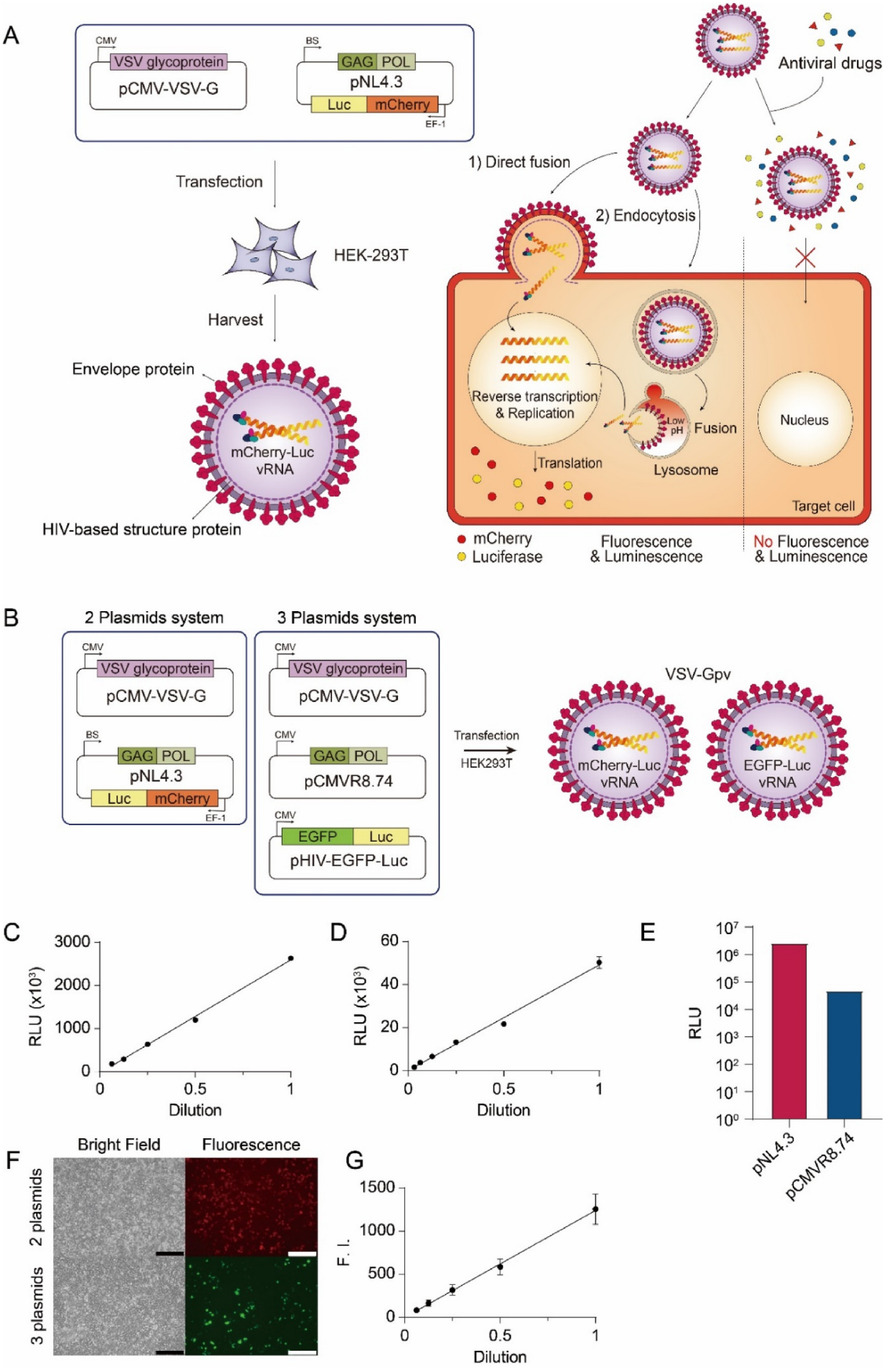
A
CMV
VSV glycoprotein
pCMV-VSV-G
BS
GAG POL
pNL4.3
Luc mCherry
EF-1
Transfection
HEK-293T
Harvest
Envelope protein
mCherry-Luc vRNA
HIV-based structure protein
Antiviral drugs
1) Direct fusion
2) Endocytosis
Reverse transcription & Replication
Low pH
Fusion
Translation
Lysosome
Nucleus
Target cell
mCherry
Luciferase
Fluorescence & Luminescence
No Fluorescence & Luminescence
B
2 Plasmids system
3 Plasmids system
pCMVR8.74
EGFP Luc
pHIV-EGFP-Luc
Transfection
HEK293T
VSV-Gpv
mCherry-Luc vRNA
EGFP-Luc vRNA
C
RLU (x10³)
Dilution
D
RLU (x10³)
Dilution
E
RLU
pNL4.3
pCMVR8.74
F
Bright Field
Fluorescence
2 plasmids
3 plasmids
G
F. I.
Dilution

E484Q, or pS-CTMut L452R/E484Q) were used, where pS-CTMut has mutations at cytoplasmic tail of spike protein. Culture media containing the transfection solution were removed, and fresh culture medium was added 8 h after transfection. At 48 h post-transfection, the supernatant containing VSVpv or SARS-2pv was harvested and filtered through a 0.45 μm filter. The filtered medium containing the pseudovirus was stored at −80 °C. When required, the pseudotyped virus was pelleted using a 20% sucrose cushion using ultra-centrifugation at 50,000 × *g* for 2 h. The supernatant and sucrose layers were removed, and the resulting viral pellets were resuspended in PBS.

Following this, target cells, HEK293T ($1 \times 10^5$ cells/well) cells for VSV-Gpv and HEK293T-ACE2 cells and HEK293T-ACE2+TMPRSS2 cells ($4 \times 10^5$ cells/well) for SARS-2pv were seeded into 24-well plates and infected with 100 μL of the serially diluted pseudotyped viruses. When required, the medium was supplemented with polybrene (5 μg/mL). After 48 h post-infection, the cells were lysed with 50 μL lysis buffer (Promega, Madison, WI, USA), and relative luminescence units (RLU) of luciferase activity were detected using the Luciferase Assay Kit (Promega). All experiments were performed at least three times and expressed as mean ± standard deviation (SDs).

### 2.4. Characterization of the pseudotyped virus

Incorporation of the spike protein in the pseudotyped virus was confirmed by western blotting and dot blotting. Both western blot and dot blot were performed using the pseudotyped virus that was concentrated through ultra-centrifugation. The pseudotyped virus was lysed by adding 1% (v/v) Triton-X 100 and mixed with 6 × SDS sample buffer. The mixtures were boiled for 10 min and subjected to SDS-PAGE and western blot. For dot blotting, pseudotyped viruses lysed with 1% (v/v) Triton-X 100 were used. Pseudotyped virus without spike protein or bovine serum albumin (BSA) was used as a pseudotyped virus negative control. Western blotting was performed with rabbit anti-SARS-CoV-2 antibody (Abcam, ab272504) at a 1:2000 dilution as the primary antibody and goat anti-rabbit IgG (Sigma Aldrich, a0545) at a 1:2000 dilution as the secondary antibody. Dot blotting was performed with laboratory-engineered anti-SARS-CoV-2 (receptor-binding domain) RBD antibody as the primary antibody and goat anti-human IgG Fc antibody (Abcam, ab97225) as the secondary antibody.

The incorporation of reporter genes, mCherry, and luciferase genes was confirmed by reverse transcription (RT)-PCR. The primer 5′-CGGCTCCTGCTTCTGAGAGGGAG-3′ was used to synthesize cDNA for the incorporated viral RNAs. The amount of cDNA was calculated using quantitative real-time (qRT)-PCR. The primers 5′-GATGACAGCATGTCAGGGAGTG-3′ and 5′-AGCCCTTTTTCCTAGGGGCC-3′ and HiPi real-time PCR 2x Master Mix with SYBR Green (Elpisbio, EBT-1802) were used according to the manufacturer's instructions.

### 2.5. Preparation of the antiviral drugs

Camostat mesylate and remdesivir were dissolved in dimethyl sulfoxide (DMSO) at a stock concentration of 100 mM. Hydroxychloroquine sulfate (HQ) was dissolved in water to a stock concentration of 100 mM. Heparin was obtained from Galen (North Haven, USA) and stored in water at a stock concentration of 1mM. Antibodies against SARS-CoV-2 were generated in the laboratory. Korean red ginseng extracts were obtained from KT&G.

### 2.6. Pseudovirus inhibition assays

The target cells for each pseudotyped virus were seeded in 24-well plates as described above. ~$2 \times 10^4$ RLU of the pseudotyped virus was used to infect each well. For the inhibition assay, 1 h before infection, cells or pseudotyped viruses were pretreated with antiviral drugs (camostat mesylate or remdesivir for cell pretreatment and heparin for pseudotyped virus pretreatment). Luciferase activity was measured 48 h after infection and the percentage of luciferase activity was calculated using GraphPad Prism software (version 6.0; GraphPad Software, San Diego, CA, USA).

## 3. Results and discussion

### 3.1. Dual reporter genes in a single plasmid enhance co-expression in infected cells

Among the many lentivirus vectors employed in the literature, three plasmids available from Addgene were compared for the pseudovirus particle production. In the two-plasmid system, all genes for packaging and dual reporters were incorporated into a single plasmid, pNL4.3 [46], which simultaneously codes for Gag-Pol proteins as well as the dual reporters luciferase and mCherry (Fig. 1B). In the three-plasmid system, plasmid pCMVR8.74 codes for Gag-Pol, whereas plasmid pHIV-EGFP-Luc encodes the dual reporters luciferase and EGFP (Fig. 1B). Two pseudovirus systems were compared using glycoproteins of vesicular stomatitis virus (VSV-G) and dual reporters (Fig. 1B). To compare the efficiency of pseudovirus production in each system, the luciferase activity was measured following transfection of HEK293T cells with two or three plasmids (Fig. 1C and D). When a reduction in luciferase activity was observed in two-fold serially diluted pseudoviruses the reduction was proportional to the dilution, regardless of whether the pseudoviruses were produced using a two-plasmid or three-plasmid system. Pseudoviruses of VSV-G (VSV-Gpv) prepared from the two-plasmid system showed 53-fold higher luciferase activity compared to that of the three-plasmid system (Fig. 1E). The titer of VSV-Gpv produced using the two-plasmid system was as high as $10^9$ RLU/mL. When fluorescence microscopic images were obtained to compare the expression of fluorescence proteins in infected cells (Fig. G) the expression of mCherry by the cells transfected with VSV-Gpv prepared using the two-plasmid system showed greater efficiency compared to that of cells transfected with VSV-Gpv expressing EGFP from the three-plasmid system. These differences in luciferase activity and fluorescence intensity are likely to arise from the transfection efficiency. The fluorescence intensity of mCherry was linearly proportional to the titer of VSV-Gpv (Fig. 1H), which is a useful feature when employed as an assay system.

VSV-Gpv, produced using the two-plasmid system, was used to assess the antiviral activity of the drugs (Fig. 2A). As pseudoviruses have been widely used to evaluate the entry-blocking activity of various drugs [47–49], we compared the activity of heparins and liposomes embedded with ganglioside (lipo-G). Heparin binds to VSV-G, thereby inhibiting infection [50]. In contrast, gangliosides are receptors for the hemagglutinin of influenza viruses [51–53]. As

**Fig. 1.** Pseudovirus system with dual reporters. (A) Schematic diagram of preparation, infection, and reporter-expression of the dual-reporter pseudovirus. (B) Comparison of plasmid components for VSV-based two- and three-plasmids systems. Luciferase activity of HEK293T cells infected by serially diluted VSV-Gpv from two- (C) or three-plasmids system (D) . (E) Comparison of luminescence of HEK293T cells infected by pseudoviruses from each system. (F) Optical and fluorescence microscopic images of infected 293T cells. Cells expressing mCherry (red) and EGFP (green) are shown. Scale bar = 250 mm. (G) Spectrophotometric measurements of fluorescence intensity (F·I.) of mCherry from cells infected by serially diluted VSV-Gpv prepared with two-plamids system.

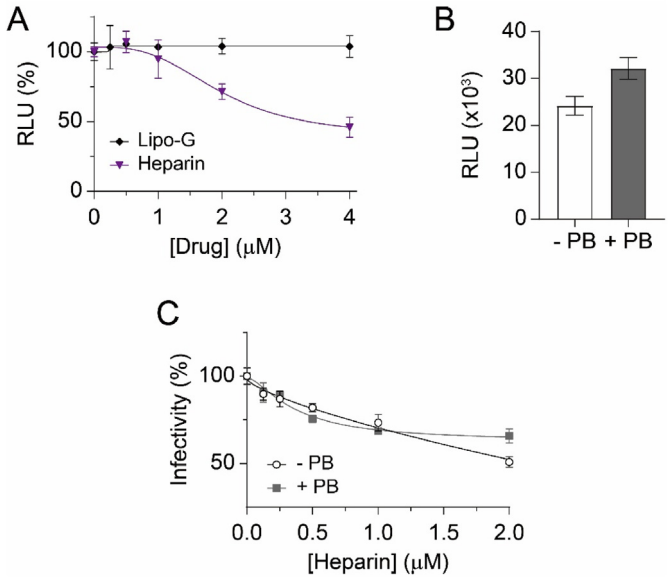


**Fig. 2.** Application of pseudovirus system with dual reporters for assessment of antivirals. (A) Luciferase activity analysis for the inhibition of pseudovirus infection by heparin and lipo-G. (B) Comparison of luciferase activity in the absence and presence of PB during infection. (C) Inhibition of pseudovirus infection with or without PB by heparin.

expected, heparin showed a moderate inhibitory effect on VSV-Gpv (54% inhibition at 4 μM), whereas lipo-G did not affect pseudovirus infection (Fig. 2A).

Polybrene (PB) facilitates viral infection via its positive charge. VSV-Gpv infection was enhanced by 33% following supplementation with PB (Fig. 2B). However, the presence of PB slightly altered the dose-response curve, thus reducing linearity (Fig. 2C). In summary, the two-plasmid system harnessing pNL4.3 enabled efficient pseudovirus production with a high titer, enabling drug screening through either of the dual reporters.

### 3.2. Pseudotyped SARS-CoV-2 with dual reporters

High-titer production of SARS-2pv was investigated through a simple process using a two-plasmid system. Plasmids pNL4.3 and pS-WT encoding dual reporters and spike (S) protein, respectively, were co-transfected to produce SARS-2pv (Fig. 3A). HEK293T cells transfected with pS-WT expressed S proteins on their membranes (Fig. 2B). However, co-transfection of pNL4.3 did not result in the incorporation of S proteins into the pseudovirus particles (Fig. 3B). Thus, two alanine mutations on the cytoplasmic tail of the S protein, which ruin the endoplasmic reticulum (ER) retrieval signal, were introduced to incorporate S proteins into the pseudovirus particles (Fig. 3C) [37]. The incorporation of these mutations into the plasmid (pS-CTMut), enabled incorporation of S proteins in the pseudovirus particles, resulting in the generation of SARS-2pv.

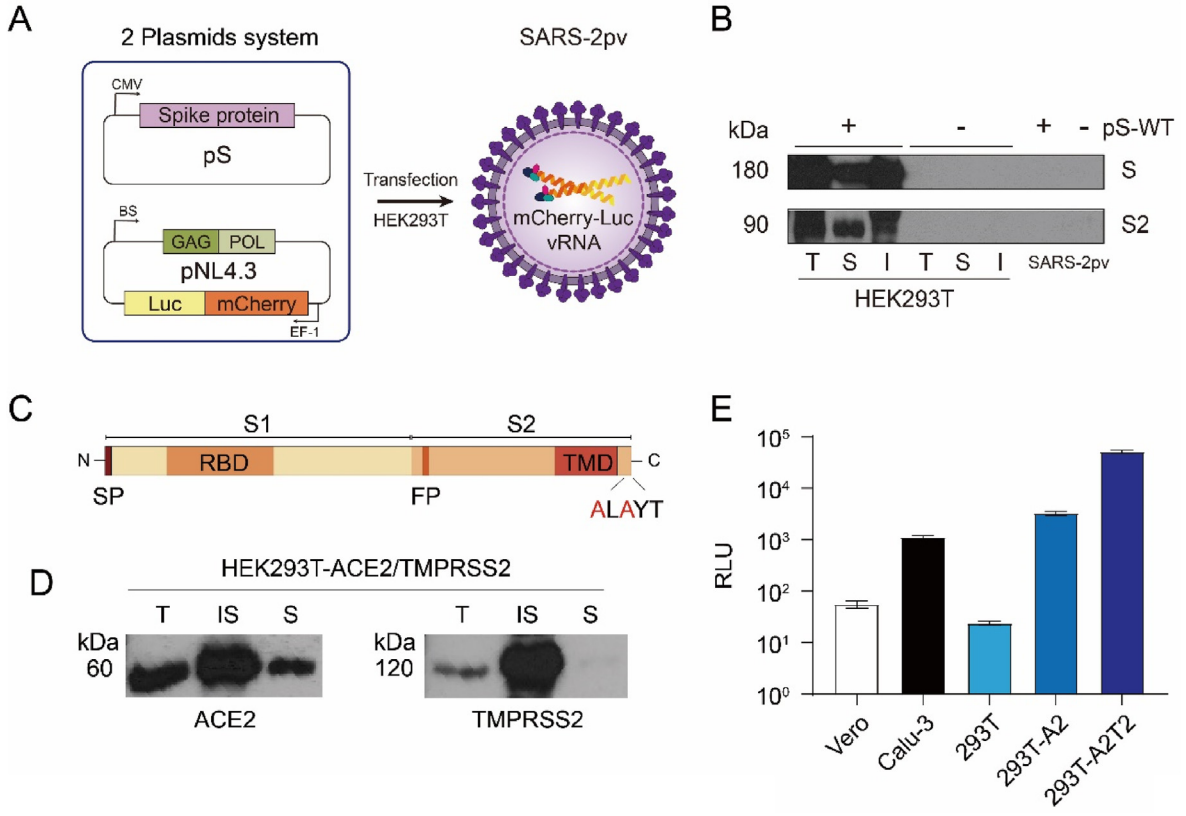


**Fig. 3.** Production and optimization of SARS-2pv through two-plasmids system. (A) Structure of plasmid constructs. Env plasmid (pS) encoding spike protein and a packaging plamid (pNL4.3) including dual reporters were used. (B) Western blot analysis for expression and incorporation of wild type S proteins. Analysis of total (T), soluble (S), and insoluble (I) fractions of HEK293T cells transfected with or without env plamids. SARS-2pv with or without env plamsids were also analyzed. Both full-length S protein and cleaved S2 protein were detected. (C) The construct of cytoplasmic tail (CT)-mutated S protein (CTΔ) are shown. Expression of signal peptide (SP), receptor binding domain (RBD), fusion peptide (FP), and transmembrane domain (TMD. The mutations on CT domain are in red. (D) Expression of ACE2 and TMPRSS2 in transfected HEK293T cells using western blotting. (E) Luminescence of various cell types following SARS-2pv infection. Vero, Calu-3, HEK293T (293T), ACE2-expressing 293T (293T-A2), and ACE2/TMPRSS2-expressing 293T (293T-A2T2) were explored.

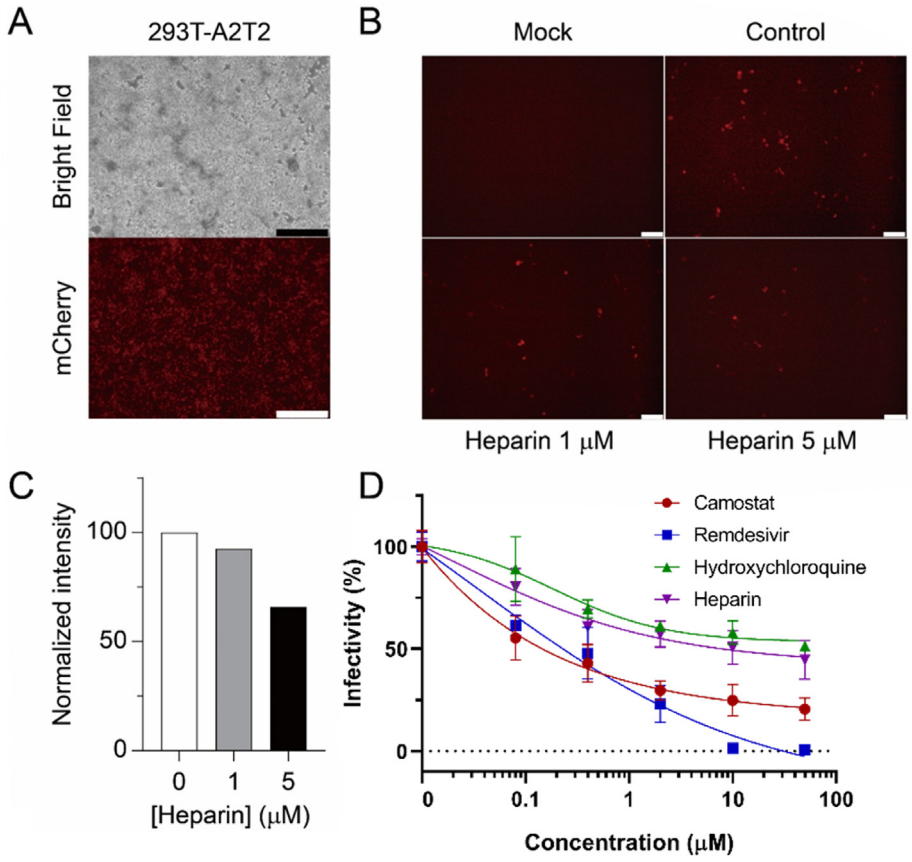


**Fig. 4.** Analysis of antiviral activity of anti-SARS-CoV-2 candidate drugs using SARS-2pv generated with two-plasmids system. (A) Optical and fluorescence microscopic images of ACE2/TMPRSS2-expressing 293T cells infected by SARS-2pv. Scale bar = 500 μm. (B) Evaluation of the inhibitory effect of heparin on pv infection using fluorescence imaging. 293T-A2T2 cells only (mock) and infected cells treated with 0 (control), 1 μM, and 5 μM of heparin. Scale bar = 100 μm. (C) Total fluorescence intensity analysis using ImageJ software. (D) Evaluation of antiviral activity of four different drugs against SARS-2pv by measuring luminescence.

The cell types were then optimized for infection with SARS-2pv from the two-plasmid system (Fig. 3D and E). First, Vero cells expressing angiotensin 2 (ACE2) only and Calu-3 cells expressing both ACE2 and TMPRSS2 were compared for their susceptibility to SARS-2pv. Calu-3 cells showed ~20-fold higher infection with SARS-2pv compared to that of Vero cells. TMPRSS2-mediated direct fusion, along with fusion in endosomes by cathepsin proteases is essential for SARS-CoV-2 infection [29,31]. As Calu-3 cells grow very slowly and require a long preparation time, HEK293T cells were tested as the infection host cells. HEK293T cells transfected with pCMV-ACE2 expressing only ACE2 were compared with cells transfected with both pCMV-ACE2 and pCMV-TMPRSS2 (Fig. 3F). HEK293T-ACE2 and HEK293T-ACE2/TMPRSS2 cells showed 2.1- and 3.3-log higher luciferase activity, respectively, compared with that of wild-type HEK293T cells. This infection efficiency was tens of times higher compared to that of the Vero and Calu-3 cells. In addition, the higher luciferase activity in HEK293T-ACE2 cells provided an opportunity to analyze the TMPRSS2-independent mechanism of infection with higher accuracy compared to that in Vero cells (Fig. 3E).

### 3.3. Antiviral assays of anti-SARS-CoV-2 drugs using SARS2-pv

The antiviral effects of several SARS-CoV-2 drugs were analyzed using SARS-2pv expressing dual reporters. First, the inhibitory activity of heparin, which electrostatically binds to the S proteins of SARS-CoV-2, was evaluated by measuring mCherry fluorescence. HEK293T-ACE2/TMPRSS2 cells infected with SARS-2pv strongly expressed mCherry protein, as observed using fluorescence microscopy (Fig. 4A). When heparin was supplemented during SARS-2pv infection, mCherry expression was reduced in a concentration-dependent manner due to entry inhibition (Fig. 4B). The total intensity of each image could be quantified using the ImageJ software (Fig. 4C).

Four repurposed drugs targeting each step of infection were tested for their antiviral activity using SARS-2pv. TMPRSS2 inhibitor (camostat) [54,55], RNA-dependent RNA polymerase (RdRp) inhibitor (remdesivir) [56,57], inhibitor of endosomal acidification (hydroxychloroquine) [58,59], and SARS-CoV-2 entry blocker (heparin) [60] were evaluated by measuring the luciferase activity of infected HEK293T-ACE2/TMPRSS2 cells (Fig. 3D). Remdesivir showed the greatest inhibitory effect, whereas hydroxychloroquine and heparin exhibited moderate activity, consistent with previous results [50–56]. These results show that the SARS-2pv with dual reporters generated in this study provides a simple and quantitative approach for the evaluation of antiviral activity of drugs by measuring fluorescence and/or luciferase activity.

### 3.4. Korean red ginseng elicits cellular resistance against SARS-CoV-2 infection

The protective effects of red ginseng against various viruses have been previously suggested [61]. Furthermore, red ginseng has been considered to possess beneficial effects against SARS-CoV-2 [62,63]. Here, we provide experimental evidence of the protective

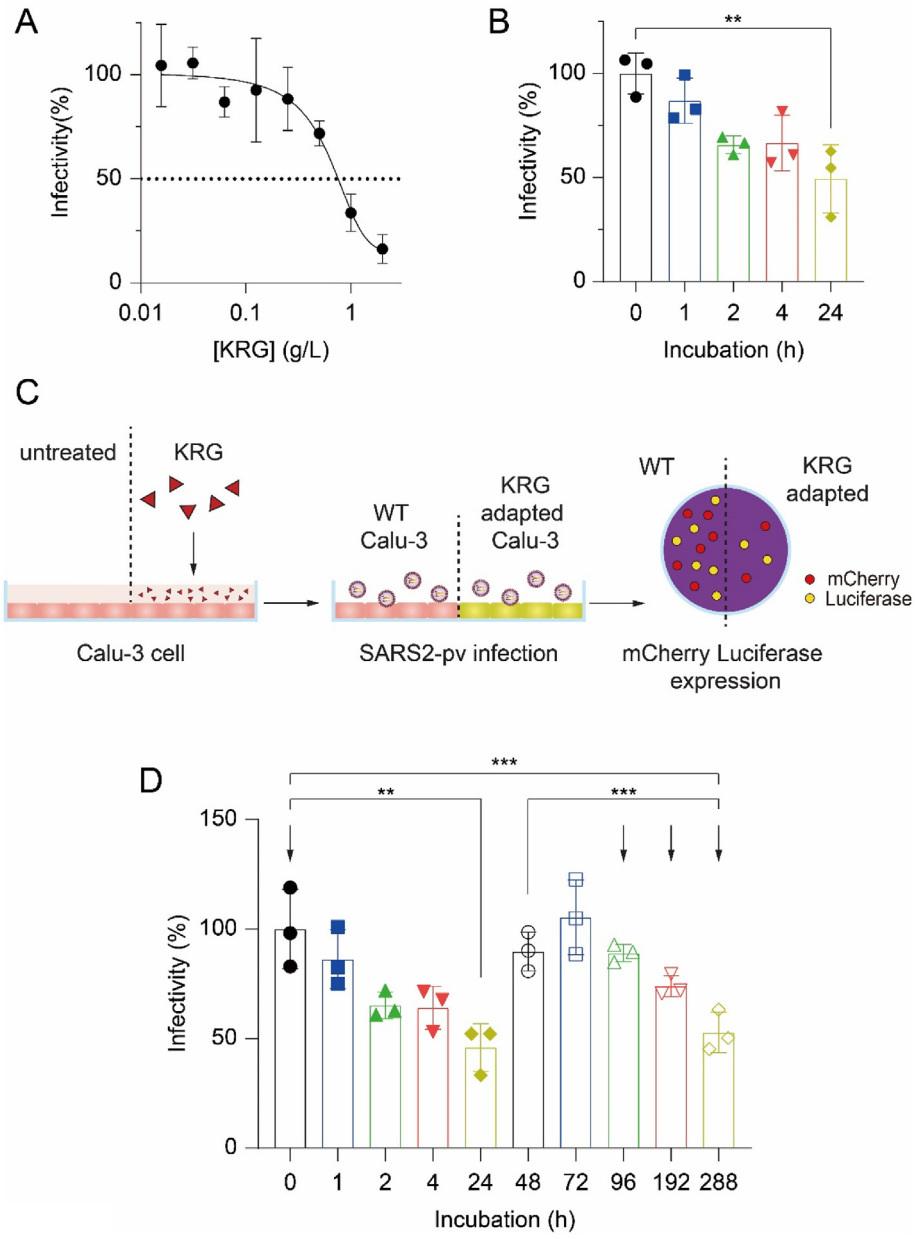


**Fig. 5.** SARS-2pv inhibition by KRG. (A) Evaluation of direct inhibitory effect of KRG extract on SARS-2pv infection in transfected HEK293T cells. (B) Analysis of infectivity of SARS-2pv on transfected HEK293T cells pre-adapted to KRG extract for 0, 1, 4, and 24 h. (C) Schematic diagram of KRG adaption assay in Calu-3 cells. (D) Analysis of infectivity of SARS-2pv on Calu-3 cells pre-adapted to KRG extract. The arrows indicate KRG treatment time points.

effect of Korean red ginseng (KRG, *Panax ginseng* Meyer) against SARS-CoV-2, using the method established above.

SARS2-pv cells were incubated with KRG extract at 37 °C for 2 h, which was then directly applied to HEK293T-ACE2-TMPRSS2 cells. Media containing SARS-2pv and KRG extract were removed after 8 h of incubation in a $CO_2$ incubator, followed by addition of fresh media. When the luciferase activity was measured following 48 h of incubation, infectivity of SARS2-pv was reduced in a concentration-dependent manner (Fig. 5A). A half inhibitory concentration of 0.75 g/L suggested a moderate inhibitory effect of KRG against SARS-CoV-2 infection. Despite this moderate antiviral effects of KRG against SARS2-pv it was unlikely that KRG would directly interact with the virus in vivo for such a prolonged period, leading to further investigation.

HEK293T-ACE2-TMPRSS2 cells were treated with 1 g/L KRG for 24 h. After removing KRG extract, the cells were infected with SARS-2pv and luciferase activity was measured following 48 h of infection. The infectivity of SARS-2pv gradually decreased depending on the KRG treatment time (Fig. 5B). Following 24 h of incubation, as high as 50% of the infection was protected even in the absence of direct interaction between the virus and KRG. This result indicated that KRG treatment elicited the resistance of cells to SARS-CoV-2 infection.

Further analyses were performed using Calu-3 cells. Calu-3 cells were treated with KRG extract (1 g/L), which was removed after the designated time, followed by SARS-2pv infection and luciferase measurement 48 h post infection. A time-dependent protective effect was consistently observed (Fig. 5C and D). Infectivity was only half that of untreated cells following 24 h of exposure to KRG.

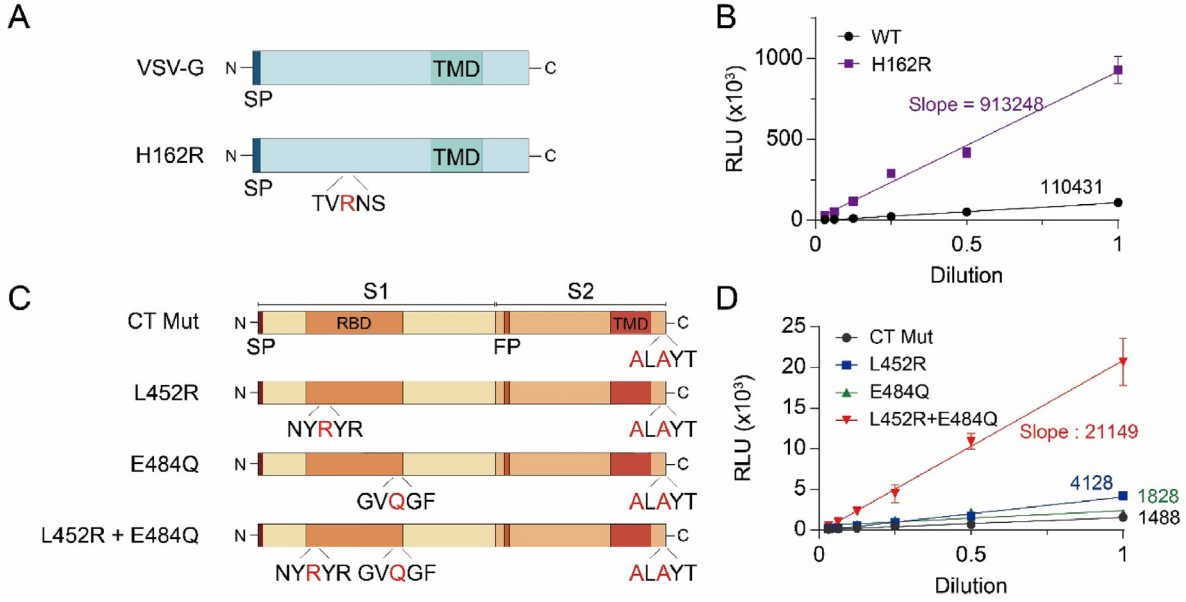


**Fig. 6.** Effect of S protein mutation of VSV-Gand SARS-2pv on infectivity. (A) Protein constructs of wild type and H162R mutated VSV-G. (B) Comparison of the infectivity of VSV-Gpv WT and H162R. Luminescence was measured from cells infected by serially diluted pseudovirus. The slope of fitter line was considered as criteria for comparison. (C) Four variants of S proteins that were incorporated to SARS-2pv. Mutations on RBD (L452R or/and E484Q) in pS-CTMut. (D) Measurement and comparison of the infectivity of variants on 293T-A2T2 cells.

Surprisingly, the protective effect was lost after 48 h of KRG treatment, suggesting that the cellular state enabling the cell resistance to virus infection returned to a normal state after a certain time of exposure to KRG. When the Calu-3 cells were treated repeatedly for 96 h, they regained protective activity against SARS-2pv infection. Thus, it is highly likely that KRG elicits a protective ability to cells against SARS-CoV-2 infection, however, further investigation is warranted to understand the molecular mechanisms by which this resistance is acquired.

### 3.5. Analysis of the infectivity of mutants

The structures of envelope proteins of SARS-CoV-2, such as the VSV-G and S proteins, determine the viral infectivity based on interactions with host receptors. Therefore, point mutations were introduced into the two pseudovirus particles to compare the effect of mutations on the viral entry of the pseudovirus. The VSV-G mutation H162R, which is located on the pH sensor domain, is known to widen the pH range of membrane fusion [64]. Consistent with previous reports, VSV-Gpv harboring the H162R mutation (Fig. 6A) showed an 8.3-fold higher luciferase activity compared to that of WT VSV-Gpv (Fig. 6B). This is likely because VSV-Gpv H162R can fuse with the endosomal membrane even at a weak acidic pH.

Many SARS-CoV-2 variants have been exposed to several mutations in their S proteins. In particular, mutations in the receptor-binding domain (RBD) have been reported to greatly increase infectivity [65,66]. Therefore, we tested whether the mutations in the established SARS-2pv showed a similar increase in infectivity (Fig. 6C). Two mutations in RBD, L452R and E484Q, were inserted into the S protein of SARS2-pv. The L452R mutation in S proteins is involved in immune evasion and results in an increased infection [65,67,68]. The E484Q mutation of S proteins increases the interaction with human ACE2 and stabilizes the conformation of RBD [69–71]. Compared to the WT SARS-2pv, the L452R variant resulted in a 2.8-fold higher luciferase activity, whereas the E484Q variant did not improve infectivity (Fig. 6D). Remarkably, when both mutations were introduced, the L452R/E484Q variant exhibited a 14.2-fold improved infectivity compared to that of WT SARS-2pv. These results suggest that the effects of mutations can be reliably reflected in the pseudovirus assay system established in this study.

## 4. Conclusion

Pseudoviruses of VSV and SARS-CoV-2 with dual reporters of fluorescence protein and luciferase were established. The SARS-2pv developed in this study were used to evaluate various antiviral agents against SARS-CoV-2. KRG, which has been considered a potential antiviral extract against various viruses, including SARS-CoV-2, showed protective effects upon pre-adaptation of cells to KRG extract. While the protective effect of KRG disappeared 24 h after treatment, repeated supplementation with KRG extract imparted cellular resistance to the virus, the mechanisms of which warrant further research. Mutations known to increase the infectivity of SARS-CoV-2 also elevated the expression of luciferase when introduced into the SARS-2pv. Thus, the SARS-2pv established in this study has been proven to act as a robust assay system for the evaluation of various antivirals, protective medicines, and viral mutations.

## Declaration of competing interest

The authors have no conflicts of interest to report.

## Acknowledgements

This study was supported by the Basic Science Research Program through the National Research Foundation of Korea (NRF), funded by the Ministry of Education (NRF-2017R1A6A1A03015642 and NRF-2020R1A2C2101964). This study was also supported by a Korean Ginseng Corporation (KGC) research grant.

## References

[1] Nie J, Huang W, Liu Q, Wang Y. HIV-1 pseudoviruses constructed in China regulatory laboratory. Emerg Microbes Infect 2020;9:32–41. https://doi.org/10.1080/22221751.2019.1702479.

[2] Cheresiz SV, Grigoryev IV, Semenova EA, Pustylnyak VO, Vlasov VV, Pokrovsky AG. A pseudovirus system for the testing of antiviral activity of compounds in different cell lines. Dokl Biochem Biophys 2010;435:295–8. https://doi.org/10.1134/S1607672910060049.

[3] Wang W, Butler EN, Veguilla V, Vassell R, Thomas JT, Moos Jr M, et al. Establishment of retroviral pseudotypes with influenza hemagglutinins from H1, H3, and H5 subtypes for sensitive and specific detection of neutralizing antibodies. J Virol Methods 2008;153:111–9. https://doi.org/10.1016/j.jviromet.2008.07.015.

[4] Zhao G, Du L, Ma C, Li Y, Li L, Poon VK, et al. A safe and convenient pseudovirus-based inhibition assay to detect neutralizing antibodies and screen for viral entry inhibitors against the novel human coronavirus MERS-CoV. Virol J 2013;10:266. https://doi.org/10.1186/1743-422X-10-266.

[5] Temperton NJ, Chan PK, Simmons G, Zambon MC, Tedder RS, Takeuchi Y, et al. Longitudinally profiling neutralizing antibody response to SARS coronavirus with pseudotypes. Emerg Infect Dis 2005;11:411–6. https://doi.org/10.3201/eid1103.040906.

[6] Chen Q, Nie J, Huang W, Jiao Y, Li L, Zhang T, et al. Development and optimization of a sensitive pseudovirus-based assay for HIV-1 neutralizing antibodies detection using A3R5 cells. Hum Vaccin Immunother 2018;14:199–208. https://doi.org/10.1080/21645515.2017.1373922.

[7] Nie J, Li Q, Wu J, Zhao C, Hao H, Liu H, et al. Establishment and validation of a pseudovirus neutralization assay for SARS-CoV-2. Emerg Microbes Infect 2020;9:680–6. https://doi.org/10.1080/22221751.2020.1743767.

[8] Du L, Zhao G, Zhang X, Liu Z, Yu H, Zheng BJ, et al. Development of a safe and convenient neutralization assay for rapid screening of influenza HA-specific neutralizing monoclonal antibodies. Biochem Biophys Res Commun 2010;397:580–5. https://doi.org/10.1016/j.bbrc.2010.05.161.

[9] Wu X, Mao Q, Yao X, Chen P, Chen X, Shao J, et al. Development and evaluation of a pseudovirus-luciferase assay for rapid and quantitative detection of neutralizing antibodies against enterovirus 71. PLoS One 2013;8:e64116. https://doi.org/10.1371/journal.pone.0064116.

[10] Nie J, Liu L, Wang Q, Chen R, Ning T, Liu Q, et al. Nipah pseudovirus system enables evaluation of vaccines in vitro and in vivo using non-BSL-4 facilities. Emerg Microbes Infect 2019;8:272–81. https://doi.org/10.1080/22221751.2019.1571871.

[11] Fan C, Wu X, Liu Q, Li Q, Liu S, Lu J, et al. A human DPP4-knockin mouse's susceptibility to infection by authentic and pseudotyped MERS-CoV. Viruses 2018;10. https://doi.org/10.3390/v10090448.

[12] Stein DR, Warner BM, Soule G, Tierney K, Frost KL, Booth S, et al. A recombinant vesicular stomatitis-based Lassa fever vaccine elicits rapid and long-term protection from lethal Lassa virus infection in Guinea pigs. NPJ Vaccines 2019;4:8. https://doi.org/10.1038/s41541-019-0104-x.

[13] Henao-Restrepo AM, Longini IM, Egger M, Dean NE, Edmunds WJ, Camacho A, et al. Efficacy and effectiveness of an rVSV-vectored vaccine expressing Ebola surface glycoprotein: interim results from the Guinea ring vaccination cluster-randomised trial. Lancet 2015;386:857–66. https://doi.org/10.1016/S0140-6736(15)61117-5.

[14] Tani H, Morikawa S, Matsuura Y. Development and applications of VSV vectors based on cell tropism. Front Microbiol 2011;2:272. https://doi.org/10.3389/fmicb.2011.00272.

[15] McKay T, Patel M, Pickles RJ, Johnson LG, Olsen JC. Influenza M2 envelope protein augments avian influenza hemagglutinin pseudotyping of lentiviral vectors. Gene Ther 2006;13:715–24. https://doi.org/10.1038/sj.gt.3302715.

[16] Goyvaerts C, De Vlaeminck Y, Escors D, Lienenklaus S, Keyaerts M, Raes G, et al. Antigen-presenting cell-targeted lentiviral vectors do not support the development of productive T-cell effector responses: implications for in vivo targeted vaccine delivery. Gene Ther 2017;24:370–5. https://doi.org/10.1038/gt.2017.30.

[17] Zhang L, Li Q, Liu Q, Huang W, Nie J, Wang Y. A bioluminescent imaging mouse model for Marburg virus based on a pseudovirus system. Hum Vaccin Immunother 2017;13:1811–7. https://doi.org/10.1080/21645515.2017.1325050.

[18] Hu D, Zhang J, Wang H, Liu S, Yu L, Sun L, et al. Chikungunya virus glycoproteins pseudotype with lentiviral vectors and reveal a broad spectrum of cellular tropism. PLoS One 2014;9:e110893. https://doi.org/10.1371/journal.pone.0110893.

[19] Ou X, Liu Y, Lei X, Li P, Mi D, Ren L, et al. Characterization of spike glycoprotein of SARS-CoV-2 on virus entry and its immune cross-reactivity with SARS-CoV. Nat Commun 2020;11:1620. https://doi.org/10.1038/s41467-020-15562-9.

[20] Nie J, Li Q, Wu J, Zhao C, Hao H, Liu H, et al. Quantification of SARS-CoV-2 neutralizing antibody by a pseudotyped virus-based assay. Nat Protoc 2020;15:3699–715. https://doi.org/10.1038/s41596-020-0394-5.

[21] Condor Capcha JM, Lambert G, Dykxhoorn DM, Salerno AG, Hare JM, Whitt MA, et al. Generation of SARS-CoV-2 spike pseudotyped virus for viral entry and neutralization assays: a 1-week protocol. Front Cardiovasc Med 2020;7:618651. https://doi.org/10.3389/fcvm.2020.618651.

[22] Barlan A, Zhao J, Sarkar MK, Li K, McCray Jr PB, Perlman S, et al. Receptor variation and susceptibility to Middle East respiratory syndrome coronavirus infection. J Virol 2014;88:4953–61. https://doi.org/10.1128/JVI.00161-14.

[23] Fukushi S, Mizutani T, Saijo M, Matsuyama S, Miyajima N, Taguchi F, et al. Vesicular stomatitis virus pseudotyped with severe acute respiratory syndrome coronavirus spike protein. J Gen Virol 2005;86(Pt 8):2269–74. https://doi.org/10.1099/vir.0.80955-0.

[24] Simmons G, Reeves JD, Rennekamp AJ, Amberg SM, Piefer AJ, Bates P. Characterization of severe acute respiratory syndrome-associated coronavirus (SARS-CoV) spike glycoprotein-mediated viral entry. Proc Natl Acad Sci U S A 2004;101:4240–5. https://doi.org/10.1073/pnas.0306446101.

[25] Takada A, Robison C, Goto H, Sanchez A, Murti KG, Whitt MA, et al. A system for functional analysis of Ebola virus glycoprotein. Proc Natl Acad Sci U S A 1997;94:14764–9. https://doi.org/10.1073/pnas.94.26.14764.

[26] Mather ST, Wright E, Scott SD, Temperton NJ. Lyophilisation of influenza, rabies and Marburg lentiviral pseudotype viruses for the development and distribution of a neutralisation -assay-based diagnostic kit. J Virol Methods 2014;210:51–8. https://doi.org/10.1016/j.jviromet.2014.09.021.

[27] Li Q, Liu Q, Huang W, Wu J, Nie J, Wang M, et al. An LASV GPC pseudotyped virus based reporter system enables evaluation of vaccines in mice under non-BSL-4 conditions. Vaccine 2017;35:5172–8. https://doi.org/10.1016/j.vaccine.2017.07.101.

[28] Desforges M, Le Coupanec A, Dubeau P, Bourgouin A, Lajoie L, Dube M, et al. Human coronaviruses and other respiratory viruses: underestimated opportunistic pathogens of the central nervous system? Viruses 2019;12. https://doi.org/10.3390/v12010014.

[29] Jackson CB, Farzan M, Chen B, Choe H. Mechanisms of SARS-CoV-2 entry into cells. Nat Rev Mol Cell Bio 2021. https://doi.org/10.1038/s41580-021-00418-x.

[30] Yang J, Petitjean SJL, Koehler M, Zhang Q, Dumitru AC, Chen W, et al. Molecular interaction and inhibition of SARS-CoV-2 binding to the ACE2 receptor. Nat Commun 2020;11:4541. https://doi.org/10.1038/s41467-020-18319-6.

[31] Hoffmann M, Kleine-Weber H, Schroeder S, Kruger N, Herrler T, Erichsen S, et al. SARS-CoV-2 cell entry depends on ACE2 and TMPRSS2 and is blocked by a clinically proven protease inhibitor. Cell 2020;181:271–80. https://doi.org/10.1016/j.cell.2020.02.052. e8.

[32] Lukassen S, Chua RL, Trefzer T, Kahn NC, Schneider MA, Muley T, et al. SARS-CoV-2 receptor ACE2 and TMPRSS2 are primarily expressed in bronchial transient secretory cells. EMBO J 2020;39:e105114. https://doi.org/10.15252/embj.20105114.

[33] Belouzard S, Chu VC, Whittaker GR. Activation of the SARS coronavirus spike protein via sequential proteolytic cleavage at two distinct sites. Proc Natl Acad Sci U S A 2009;106:5871–6. https://doi.org/10.1073/pnas.0809524106.

[34] Johnson BA, Hage A, Kalveram B, Mears M, Plante JA, Rodriguez SE, et al. Peptidoglycan-Associated cyclic lipopeptide disrupts viral infectivity. J Virol 2019;93. https://doi.org/10.1128/JVI.01282-19.

[35] Follis KE, York J, Nunberg JH. Furin cleavage of the SARS coronavirus spike glycoprotein enhances cell-cell fusion but does not affect virion entry. Virology 2006;350:358–69. https://doi.org/10.1016/j.virol.2006.02.003.

[36] Millet JK, Whittaker GR. Host cell proteases: critical determinants of coronavirus tropism and pathogenesis. Virus Res 2015;202:120–34. https://doi.org/10.1016/j.virusres.2014.11.021.

[37] Hu J, Gao Q, He C, Huang A, Tang N, Wang K. Development of cell-based pseudovirus entry assay to identify potential viral entry inhibitors and neutralizing antibodies against SARS-CoV-2. Genes Dis 2020;7:551–7. https://doi.org/10.1016/j.gendis.2020.07.006.

[38] Huang SW, Tai CH, Hsu YM, Cheng D, Hung SJ, Chai KM, et al. Assessing the application of a pseudovirus system for emerging SARS-CoV-2 and re-emerging avian influenza virus H5 subtypes in vaccine development. Biomed J 2020;43:375–87. https://doi.org/10.1016/j.bj.2020.06.003.

[39] Tani H, Kimura M, Tan L, Yoshida Y, Ozawa T, Kishi H, et al. Evaluation of SARS-CoV-2 neutralizing antibodies using a vesicular stomatitis virus possessing SARS-CoV-2 spike protein. Virol J 2021;18:16. https://doi.org/10.1186/s12985-021-01490-7.

[40] Xiong HL, Wu YT, Cao JL, Yang R, Liu YX, Ma J, et al. Robust neutralization assay based on SARS-CoV-2 S-protein-bearing vesicular stomatitis virus (VSV) pseudovirus and ACE2-overexpressing BHK21 cells. Emerg Microbes Infect 2020;9:2105–13. https://doi.org/10.1080/22221751.2020.1815589.

[41] Yang R, Huang B, A R, Li W, Wang W, Deng Y, et al. Development and effectiveness of pseudotyped SARS-CoV-2 system as determined by neutralizing efficiency and entry inhibition test in vitro. Biosaf Health 2020;2:226–31. https://doi.org/10.1016/j.bsheal.2020.08.004.

[42] Yang P, Yang Y, Wu Y, Huang C, Ding Y, Wang X, et al. An optimized and robust SARS-CoV-2 pseudovirus system for viral entry research. J Virol Methods 2021;295:114221. https://doi.org/10.1016/j.jviromet.2021.114221.

[43] Li QQ, Liu Q, Huang WJ, Li XG, Wang YC. Current status on the development of pseudoviruses for enveloped viruses. Rev Med Virol 2018;28. https://doi.org/10.1002/rmv.1963.

[44] Chen M, Zhang XE. Construction and applications of SARS-CoV-2 pseudoviruses: a mini review. Int J Biol Sci 2021;17:1574–80. https://doi.org/10.7150/ijbs.59184.

[45] Hu J, Gao Q, He C, Huang A, Tang N, Wang K. Development of cell-based pseudovirus entry assay to identify potential viral entry inhibitors and neutralizing antibodies against SARS-CoV-2. Genes & Diseases 2020;7:551–7. https://doi.org/10.1016/j.gendis.2020.07.006.

[46] Lassen KG, Hebbeler AM, Bhattacharyya D, Lobritz MA, Greene WC. A flexible model of HIV-1 latency permitting evaluation of many primary CD4 T-cell reservoirs. PLoS One 2012;7:e30176. https://doi.org/10.1371/journal.pone.0030176.

[47] Bojadzic D, Alcazar O, Chen J, Chuang ST, Condor Capcha JM, Shehadeh LA, et al. Small-molecule inhibitors of the coronavirus spike: ACE2 protein-protein interaction as blockers of viral attachment and entry for SARS-CoV-2. ACS Infect Dis 2021;7:1519–34. https://doi.org/10.1021/acsinfecdis.1c00070.

[48] Wu W, Lin D, Shen X, Li F, Fang Y, Li K, et al. New influenza A Virus entry inhibitors derived from the viral fusion peptides. PLoS One 2015;10:e0138426. https://doi.org/10.1371/journal.pone.0138426.

[49] Lin D, Luo Y, Yang G, Li F, Xie X, Chen D, et al. Potent influenza A virus entry inhibitors targeting a conserved region of hemagglutinin. Biochem Pharmacol 2017;144. https://doi.org/10.1016/j.bcp.2017.07.023. 35-5.

[50] Guibinga GH, Miyanohara A, Esko JD, Friedmann T. Cell surface heparan sulfate is a receptor for attachment of envelope protein-free retrovirus-like particles and VSV-G pseudotyped MLV-derived retrovirus vectors to target cells. Molecular Therapy 2002;5:538–46. https://doi.org/10.1006/mthe.2002.0578.

[51] Kong B, Moon S, Kim Y, Heo P, Jung Y, Yu SH, et al. Virucidal nano-perforator of viral membrane trapping viral RNAs in the endosome. Nat Commun 2019;10:185. https://doi.org/10.1038/s41467-018-08138-1.

[52] Berselli GB, Sarangi NK, Gimenez AV, Murphy PV, Keyes TE. Microcavity array supported lipid bilayer models of ganglioside - influenza hemagglutinin1 binding. Chem Commun (Camb) 2020;56:11251–4. https://doi.org/10.1039/d0cc04276e.

[53] Bukrinskaia AG, Kornilaeva GV, Vorkunova NK, Timofeeva NG, Shaposhnikova GI. Gangliosides–specific receptors for the influenza virus. Vopr Virusol 1982;27:661–6.

[54] Hempel T, Raich L, Olsson S, Azouz NP, Klingler AM, Hoffmann M, et al. Molecular mechanism of inhibiting the SARS-CoV-2 cell entry facilitator TMPRSS2 with camostat and nafamostat. Chem Sci 2021;12:983–92. https://doi.org/10.1039/d0sc05064d.

[55] Sasaki M, Uemura K, Sato A, Toba S, Sanaki T, Maenaka K, et al. SARS-CoV-2 variants with mutations at the S1/S2 cleavage site are generated in vitro during propagation in TMPRSS2-deficient cells. Plos Pathog 2021;17. https://doi.org/10.1371/journal.ppat.1009233.

[56] Kokic G, Hillen HS, Tegunov D, Dienemann C, Seitz F, Schmitzova J, et al. Mechanism of SARS-CoV-2 polymerase stalling by remdesivir. Nat Commun 2021;12:279. https://doi.org/10.1038/s41467-020-20542-0.

[57] Pruijssers AJ, George AS, Schafer A, Leist SR, Gralinksi LE, Dinnon 3rd KH, et al. Remdesivir inhibits SARS-CoV-2 in human lung cells and chimeric SARS-CoV expressing the SARS-CoV-2 RNA polymerase in mice. Cell Rep 2020;32:107940. https://doi.org/10.1016/j.celrep.2020.107940.

[58] Ou TL, Mou HH, Zhang LZ, Ojha A, Choe H, Farzan M. Hydroxychloroquine-mediated inhibition of SARS-CoV-2 entry is attenuated by TMPRSS2. Plos Pathog 2021;17. https://doi.org/10.1371.

[59] Liu J, Cao RY, Xu MY, Wang X, Zhang HY, Hu HR, et al. Hydroxychloroquine, a less toxic derivative of chloroquine, is effective in inhibiting SARS-CoV-2 infection in vitro. Cell Discov 2020;6. https://doi.org/10.1038/s41421-020-0156-0.

[60] Kwon PS, Oh H, Kwon SJ, Jin W, Zhang F, Fraser K, et al. Sulfated polysaccharides effectively inhibit SARS-CoV-2 in vitro. Cell Discov 2020;6:50. https://doi.org/10.1038/s41421-020-00192-8.

[61] Im K, Kim J, Min H. Ginseng, the natural effectual antiviral: protective effects of Korean Red Ginseng against viral infection. J Ginseng Res 2016;40:309–14. https://doi.org/10.1016/j.jgr.2015.09.002.

[62] Ratan ZA, Rabbi Mashrur F, Runa NJ, Kwon KW, Hosseinzadeh H, Cho JY. Ginseng, a promising choice for SARS-COV-2: a mini review. J Ginseng Res 2022;46:183–7. https://doi.org/10.1016/j.jgr.2022.01.004.

[63] Jung EM, Lee GS. Korean Red Ginseng, a regulator of NLRP3 inflammasome, in the COVID-19 pandemic. J Ginseng Res 2022. https://doi.org/10.1016/j.jgr.2022.02.003.

[64] Zhu D, Lam DH, Yi Purwanti, Goh SL, Wu C, Zeng J, et al. Systemic delivery of fusogenic membrane glycoprotein-expressing neural stem cells to selectively kill tumor cells. Mol Ther 2013;21:1621–30. https://doi.org/10.1038/mt.2013.123.

[65] Cherian S, Potdar V, Jadhav S, Yadav P, Gupta N, Das M, et al. SARS-CoV-2 spike mutations, L452R, T478K, E484Q and P681R, in the second wave of COVID-19 in Maharashtra, India. Microorganisms 2021;9. https://doi.org/10.3390/microorganisms9071542.

[66] Liu Z, VanBlargan LA, Bloyet LM, Rothlauf PW, Chen RE, Stumpf S, et al. Identification of SARS-CoV-2 spike mutations that attenuate monoclonal and serum antibody neutralization. Cell Host Microbe 2021;29:477–88. https://doi.org/10.1016/j.chom.2021.01.014. e4.

[67] Motozono C, Toyoda M, Zahradnik J, Saito A, Nasser H, Tan TS, et al. SARS-CoV-2 spike L452R variant evades cellular immunity and increases infectivity. Cell Host Microbe 2021;29:1124–36. https://doi.org/10.1016/j.chom.2021.06.006. e11.

[68] Deng X, Garcia-Knight MA, Khalid MM, Servellita V, Wang C, Morris MK, et al. Transmission, infectivity, and neutralization of a spike L452R SARS-CoV-2 variant. Cell 2021;184:3426–37. https://doi.org/10.1016/j.cell.2021.04.025. e8.

[69] Lan J, Ge J, Yu J, Shan S, Zhou H, Fan S, et al. Structure of the SARS-CoV-2 spike receptor-binding domain bound to the ACE2 receptor. Nature 2020;581:215–20. https://doi.org/10.1038/s41586-020-2180-5.

[70] Gobeil SM, Janowska K, McDowell S, Mansouri K, Parks R, Stalls V, et al. Effect of natural mutations of SARS-CoV-2 on spike structure, conformation, and antigenicity. Science 2021;373. https://doi.org/10.1126/science.abi6226.

[71] Kumar V, Singh J, Hasnain SE, Sundar D. Possible link between higher transmissibility of Alpha, Kappa and Delta variants of SARS-CoV-2 and increased structural stability of its spike protein and hACE2 affinity. Int J Mol Sci 2021;22. https://doi.org/10.3390/ijms22179131.